University of Bristol, Centre for Doctoral Training in Quantum Engineering

An Introduction to Loss Tolerant Tree Encoding for Large Scale Linear Optical Quantum Computing

Individual Project B Report*

Sam Morley-Short†

September 16th 2015

"Don't it always seem to go, that you don't know what you've got, till it's gone."

– Joni Mitchell, *Big Yellow Taxi*

Contents

*Submitted as assessment for a three month research project postgraduate course. Supervisor: Hugo Cable

†*sam.morley-short@bristol.ac.uk*

1 Introduction

One of the main challenges facing linear optical quantum computing (LOQC) is loss. Each implementation of LOQC suffers some significant degree of loss, be it from reflective bulk optics, interfaces in fibre networks, or scattering and free-carrier absorption in integrated devices. For fault tolerant, measurement-based quantum computation one typically requires a large, highly entangled qubit lattice on which quantum error correction is performed. While such schemes can account for certain loss levels [1–3], these thresholds are still too low for practical use. To overcome this loss-tolerant protocols must be developed.

In this report we shall therefore investigate a modern loss-tolerance scheme proposed by Varnava, Browne and Rudolph, known as *counterfactual error correction*. For such we shall specifically consider photonic implementations. To provide a complete understanding of the scheme, the prerequisite theory will also be revised. The report is hence structured as follows: Section 2 provides a brief introduction to measurement-based quantum computing (MBQC) and the cluster state picture; Section 3 shall introduce the stabiliser formalism and its use for efficiently describing cluster states; Section 4 describes modern approaches to constructing cluster states; Section 5 then details the loss tolerant scheme in question; Lastly Section 6 concludes by offering some areas for further research towards practical implementation of the scheme.

2 Measurement-based quantum computing and cluster states

In general, quantum computing requires the preparation of arbitrary states. For a single qubit $|\psi\rangle$, a general state rotation $U(\theta)$ can be performed by three consecutive Euler rotations by angles α, β, γ, such that $U(\theta) = U_Z(\gamma)U_X(\beta)U_Z(\alpha) = HHU_Z(\gamma)HU_Z(\beta)HU_Z(\alpha)$ (given $U_X = HU_ZH$, where H is the Hadamard gate). Represented in the quantum circuit picture:

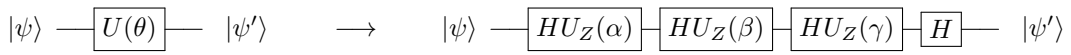

To perform these individual Hadamard plus rotation gates, a teleportation protocol combined with feed forward can be used:

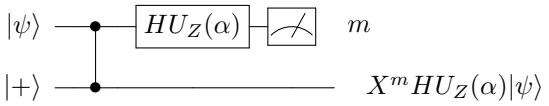

where $|+\rangle = \frac{1}{\sqrt{2}}(|0\rangle + |1\rangle)$ and $m = \{0, 1\}$ is the result of a computational basis (CB) measurement. The specific value of m determines whether the circuit need be corrected via an additional X rotation, after producing the desired output state. To perform the complete arbitrary qubit rotation, three teleportations and measurements can then be combined:

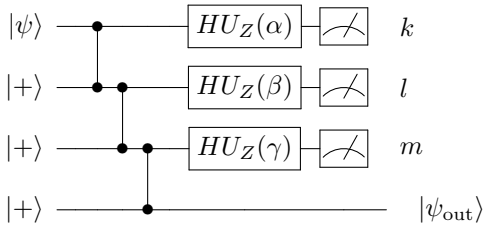

where $|\psi_{\text{out}}\rangle = (X^m HU_Z(\alpha))(X^l HU_Z(\beta))(X^k HU_Z(\gamma))|\psi\rangle$, from which $|\psi'\rangle = U_Z(\gamma)U_X(\beta)U_Z(\alpha)|\psi\rangle$ can be retrieved by applying a series of H and X gates dependant on the measurement results k, l and m . For obvious reasons, this method of quantum computation is known as, measurement-based quantum computing (MBQC). Given that $U(\theta)$ performs an arbitrary qubit rotation, one is free to set $|\psi\rangle = |+\rangle$ and represent the pre-rotation resource state as a four node linear *cluster state*:

where the nodes (◯) and edges (—) respectively represent the ($|+\rangle$) qubits and the (CZ) entanglement between them. The rotation protocol can now be depicted as:

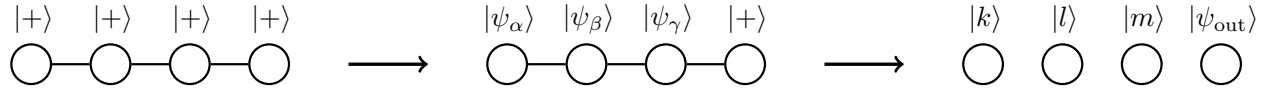

1) Initialise cluster state 2) Rotate qubits 3) Measure in CB

where $|\psi_\theta\rangle = HU_Z(\theta)|+\rangle$ in the second stage. Note: the states depicted above each cluster state node are not separable, e.g in 2) the total cluster state is not given by $|\psi_\alpha\rangle\otimes|\psi_\beta\rangle\otimes|\psi_\gamma\rangle\otimes|+\rangle$, but rather each label gives the state of each qubit had the CZ's not been performed. The results of the CB measurements are then be used to retrieve $|\psi'\rangle$ as before. This protocol can easily be extended to arbitrary multiqubit rotations. For example the arbitrary two-qubit rotation can be produced via cluster states:

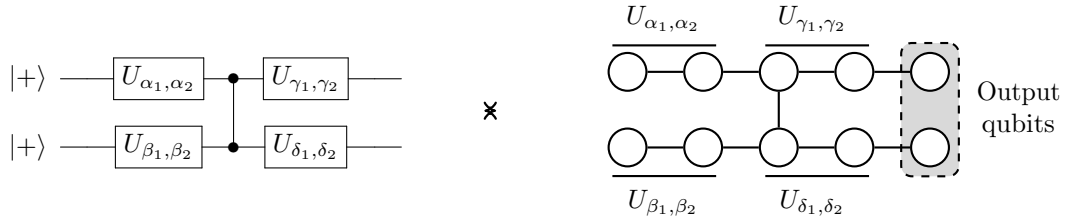

This two-qubit entangling protocol is the last requirement to perform universal quantum computation, that is, using MBQC we can perform both unitary single qubit rotations and multi-qubit entangling operations. Furthermore one key advantages to this approach is that all rotations are performed deterministically once the initial resource state has been built (which can be done efficiently). This is particularly useful for photonic applications as it removes the need for the probabilistic simulation of nonlinearities required for entanglement operations. MBQC on cluster states allows the probabilistic nature of entanglement to be addressed prior to the quantum computation, significantly reducing the failure rate of any photonic implementation.

3 Stabilizers

Gottesman-Knill theorem states that any quantum circuit using only:

i) preparation of qubits in computational basis states ($|0\rangle$ and $|1\rangle$),

ii) quantum gates from the Clifford group[1] (H, CZ and S)[2],

iii) measurements in the computational basis,

can be simulated efficiently using a classical computer and is known as a stabilizer circuit. Any n-qubit state $|\psi_S\rangle$ produced by a stabilizer circuit (known as a stabilizer state) can be uniquely defined by its stabilizers $\{S_j\}$ such that

$$S_j|\psi_S\rangle = |\psi_S\rangle \quad \forall\, j\,,\ S_j \in \mathcal{P}_n \tag{1}$$

where the Pauli group $\mathcal{P}_n$ is the group of all n-fold tensor product of Pauli operators including ± 1 and $\pm i$ multiplicative factors. In general to uniquely specify *any* n-qubit quantum state $|\psi\rangle$, 2^{2n} stabilizers would be needed, however stabilizer states $|\psi_S\rangle$ require only n (whereas conventionally 2^n vector amplitudes are required). Conveniently, the set of cluster states are contained within group of states that can be described efficiently by stabilizers, making them significantly easier to study and understand.

3.1 Transformations using stabilizers

One can find stabilizers of the state $|\psi'\rangle = U|\psi\rangle$ by transforming the stabilizers of $|\psi\rangle$ (Stab$\{|\psi\rangle\}$) by $S_j \to US_jU^\dagger$. Furthermore, given that the unitary transformation U can be constructed using only Clifford gates, the resultant state will also be a stabilizer state. For example, consider the stabilizers of two unentangled qubits both in the $|+\rangle$ state, that is $|\psi\rangle = |+\rangle_1\otimes|+\rangle_2 \equiv |++\rangle_{12}$. It is easy to see that these qubits are both stabilized by the Pauli operator $X = |+\rangle\langle+| - |-\rangle\langle-|$, that is Stab$\{|\psi\rangle\} = \{X_1\mathbb{I}_2, \mathbb{I}_1X_2\} \equiv \{X_1, X_2\}$. Consider now the entanglement of said qubits to a two qubit linear cluster state via the CZ operation $\left|\Psi_2^{\text{lin}}\right\rangle = \text{CZ}_{12}|++\rangle_{12}$. The new stabilizers are therefore given by

$$\text{Stab}\{\left|\Psi_2^{\text{lin}}\right\rangle\} = \{\text{CZ}_{12}X_1\text{CZ}_{12}, \text{CZ}_{12}X_2\text{CZ}_{12}\} = \{X_1Z_2, Z_1X_2\}\,. \tag{2}$$

Comparing these to the associated state vector

$$\left|\Psi_2^{\text{lin}}\right\rangle = \frac{1}{2}(|++\rangle + |+-\rangle + |-+\rangle - |--\rangle)_{12} = \frac{1}{\sqrt{2}}(|0+\rangle + |1-\rangle)_{12} = \frac{1}{\sqrt{2}}(|+0\rangle + |-1\rangle)_{12} \tag{3}$$

[1] Formally, the Clifford group $\mathcal{C}$ is defined as the group of operators that leave the Pauli group invariant, that is $\forall\, C \in \mathcal{C}$ and P, $P' \in \mathcal{P}_N \Rightarrow CPC^\dagger = P'$.

[2] Where S is the phase gate $|0\rangle\langle 0| + i|1\rangle\langle 1|$.

it is easy to see that these operators indeed stabilize the resultant state. Clearly however, as we progressively increase the size of our cluster, it will become increasingly unwieldy to describe in a state vector form. Fortunately, given the graph representation of any cluster state, the stabilizers associated with each qubit j are given simply by

$$S_j = X_j \prod_{k \in n(j)} Z_k \tag{4}$$

where $n(j)$ is the 'neighbourhood' of j, i.e the set of qubits directly connected to j (by CZ operations).

Also it can be further shown that any n-qubit stabilizer state $|\psi_S\rangle$ is LC-equivalent to a cluster state $|\psi_C\rangle$. That is $|\psi_S\rangle = U|\psi_C\rangle$ given $U \in \mathcal{C}_L$ where $\mathcal{C}_L$ denotes the local Clifford group (the n-fold tensor product of the set of single-qubit Clifford operations $\{H, S\}$). Therefore in the following discussion "cluster states" and "stabilizer states" can be used equivalently.

It is also important to understand the destructive and constructive operations that can be performed on cluster states and their associated stabilizer representation. For brevity, we shall only consider the effect of these operations within the cluster state picture[3].

3.2 Measurements on cluster states

When measuring cluster states, to find the resultant set of stabilizers S' from the original set S there are three procedural steps to follow [4]:

1) Replace operators with the eigenvalue of the commuting observable.

2) Remove operators from S which do not commute with observables and add stabilizers for the measured qubits.

3) Manipulate the remaining stabilizers through multiplication and local operations to retrieve cluster state form of S'.

To illustrate this process, consider the following example: We have a 5-qubit linear cluster on which we perform a Z measurement on the central qubit. Following the above procedure we can manipulate the the stabilizers and visualise this process as:

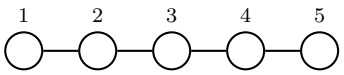

i) Initial cluster state

$S_1 = X_1\ Z_2$
$S_2 = Z_1\ X_2\ Z_3$
$S_3 = \quad Z_2\ X_3\ Z_4$
$S_4 = \quad\ Z_3\ X_4\ Z_5$
$S_5 = \quad\ \ Z_4\ X_5$

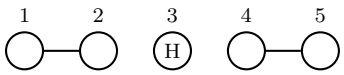

ii) Apply steps 1) and 2)

$S_1 = \quad\ \ X_1\ Z_2$
$S_2' = (-1)^{m_3}\ Z_1\ X_2$
$S_3' = (-1)^{m_3} \quad\ Z_3$
$S_4' = (-1)^{m_3} \quad\ \ X_4\ Z_5$
$S_5 = \quad\ \ Z_4\ X_5$

iii) Apply step 3)

$S_1 = \quad\ \ X_1\ Z_2$
$S_2' = (-1)^{m_3}\ Z_1\ X_2$
$S_3'' = (-1)^{m_3} \quad\ X_3$
$S_4' = (-1)^{m_3} \quad\ \ X_4\ Z_5$
$S_5 = \quad\ \ Z_4\ X_5$

where $m_3 = \{0, 1\}$ denotes the measurement outcome and $(-1)^{m_i}$ represents the result of the measurement outcome on the rest of the cluster. Here the state depicted in step ii) represents the state of cluster state after a Hadamard applied to qubit 3. Hence in iii) the state was manipulated by applying H_3 to counteract this deviation from the ideal cluster (using $HZH = X$).

Similarly, we can apply the same procedure for an X measurement on qubit 3:

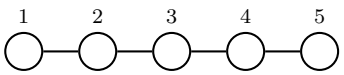

i) Initial cluster state

$S_1 = X_1\ Z_2$
$S_2 = Z_1\ X_2\ Z_3$
$S_3 = \quad Z_2\ X_3\ Z_4$
$S_4 = \quad\ Z_3\ X_4\ Z_5$
$S_5 = \quad\ \ Z_4\ X_5$

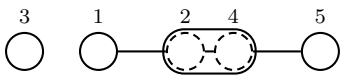

ii) Apply steps 1) and 2)

$S_3' = (-1)^{m_3}\ X_3$
$S_1 = \quad\ \ X_1\ Z_2$
$S_2' = (-1)^{m_3} \quad\ Z_2\ Z_4$
$S_4' = \quad\ \ Z_1\ X_2\ X_4\ Z_5$
$S_5 = \quad\ \ Z_4\ X_5$

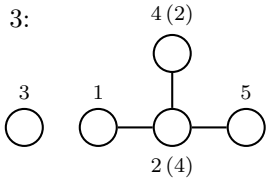

iii) Apply step 3)

$S_3' = (-1)^{m_3}\ X_3$
$S_1 = \quad\ \ X_1\ Z_2$
$S_2'' = (-1)^{m_3} \quad\ Z_2\ X_4$
$S_4'' = \quad\ \ Z_1\ X_2\ Z_4\ Z_5$
$S_5' = (-1)^{m_3} \quad\ Z_2 \quad\ X_5$

[3]For a description of the following in greater detail, please see the author's previous work on the subject.

where $S_4' = S_2 \cdot S_4$, $S_5' = S_2' \cdot S_5$ and S_2'', S_4'' were altered by applying H_4. Here we have also made use of the fact that the product of two stabilizers for a given state is also a stabilizer. Bracketed is the alternate state of the cluster had H_2 been applied (with subscripts 2 and 4 also swapped in the stabilizers). The two-qubit object depicted in ii) depicts a "redundantly encoded" qubit. This represents a correlated two qubit state that we can re-encode (e.g. $|00\rangle_{24} \rightarrow |0\rangle_{24}$ and $|11\rangle_{24} \rightarrow |1\rangle_{24}$) as a single node in the cluster state representation. Furthermore at stage ii) if an X measurement is now applied to qubit 2 (4), this would remove the qubit leaving the three qubit linear cluster of qubits 1, 4 and 5 (1, 2 and 5). In the graph state picture this can be represented as removing the measured qubit and then linking all of the qubits in it's neighbourhood together.

The effect of the different measurements are summarised below, including measurement in the Y basis omitted for brevity above:

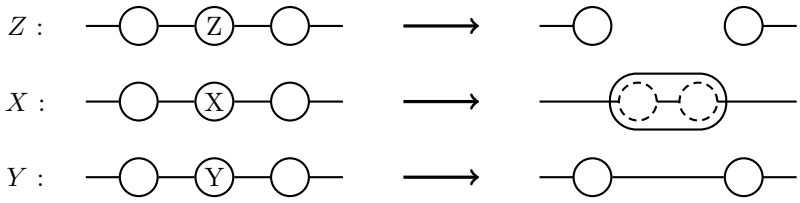

Note that these resultant states are those after manipulation into a cluster state form, i.e. they are LC-equivalent to the state produced directly after measurement.

4 Constructing cluster states

Although cluster states are traditionally introduced as $|+\rangle$ qubit nodes connected via CZ operations, this is rarely how they are actually built. Due to the probabilistic nature of entangling CZ operations in linear optics schemes, the chance of applying many successfully becomes vanishingly small. Alternatively, many resources can be consumed to achieve a high success probability, though here the scalings are generally impractical. For example, in the original Knill, Laflamme and Milburn (KLM) scheme a single CZ operating with a 95% success rate would required 10^4 (perfect) gate operations and the consumption of 1300 Bell states and 620 other ancillary states [6].

Modern approaches to constructing large cluster states require the repeated linking of small 'resource' entangled states (such as GHZ states) through Bell-like measurements known as "fusion gates" [5]. These gates have two varieties, namely Type-I and Type-II fusion, depicted in a photonic implementation in Figure 1. We shall not discuss the specific details of either gate's operation here, but rather give their operation in the cluster state picture[4]. While both gates still operate probabilistically (with a 50% success rate), this is significantly better than that of a KLM CZ gate (such as a 25% successful CZ which still requires four ancillary photons and significantly more constituent gate operations).

[4]For a detailed description fusion gate operation please see the author's previous work on the subject.

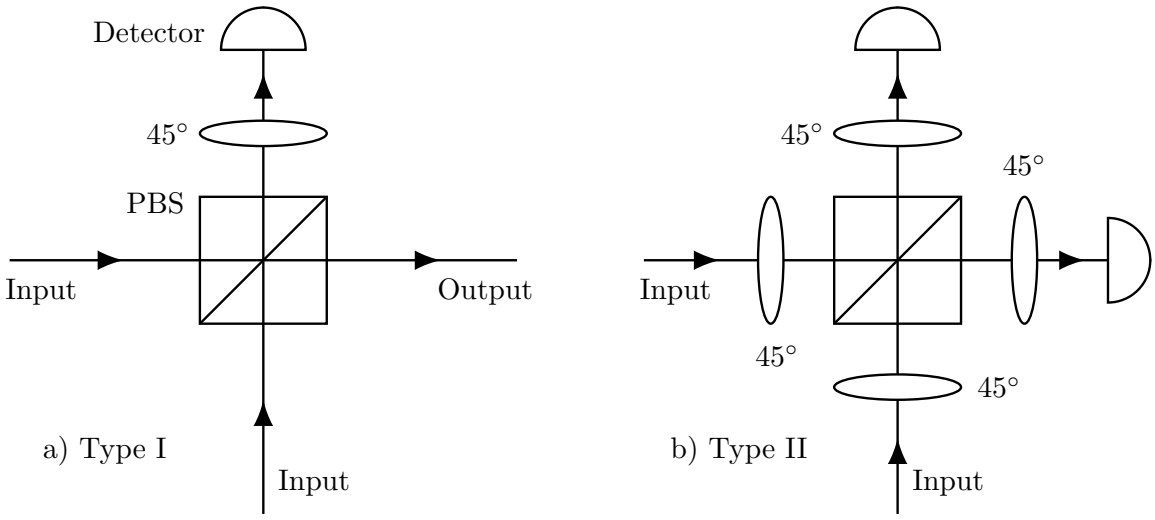

Figure 1: The two types of fusion gate for polarisation encoded $|+\rangle = \frac{1}{\sqrt{2}}(|H\rangle + |V\rangle)$ qubits. Image adapted from [5].

4.1 Type-I Fusion

When successful Type-I fusion takes two input cluster photons[5], measuring one, and outputting the other as a qubit node in the joined cluster. Failure for Type-I fusion occurs when both or neither qubits are measured at the detector. Typically in fusion operations, one is either attempting to join the ends of two linear clusters to form a longer linear cluster, or to join linear cluster midpoints to form a higher dimensional cluster structure. In the graph state picture, success joins the two clusters with the output qubit as the central node, whereas failure performs a Z-measurement on both qubits, eliminating them from the cluster. Pictorially, these are depicted as follows:

Lengthening linear clusters:

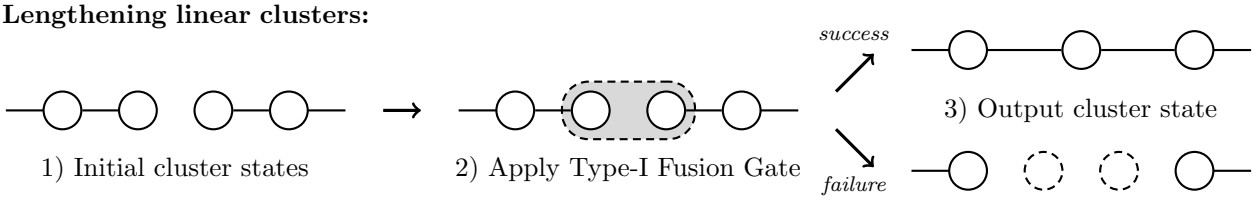

Forming multidimensional clusters:

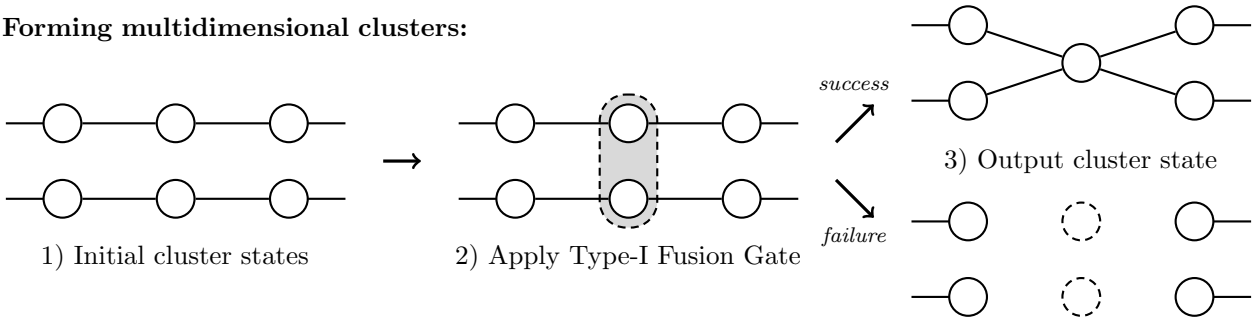

4.2 Type-II Fusion

In Type-II fusion, two photons are again input and detectors are placed on both arms. Here photon anti-bunching indicates successful operations and photon bunching indicates failure. On success, both qubits are removed, linking qubits in the neighbourhood of *both* qubits together. In the case that one of these qubits is a redundantly encoded qubit (or equivalently an input qubit linked to only a single other), this transfers all the measured qubits' links to said qubit. On failure, an X measurement is effectively performed on the input qubits. Pictorially, these are depicted as follows:

Lengthening linear clusters:

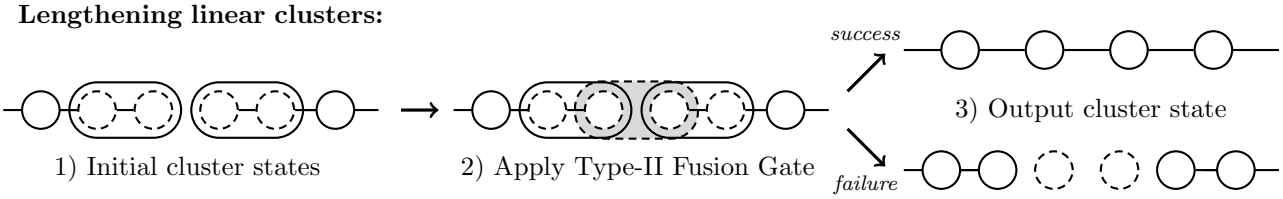

Forming multidimensional clusters:

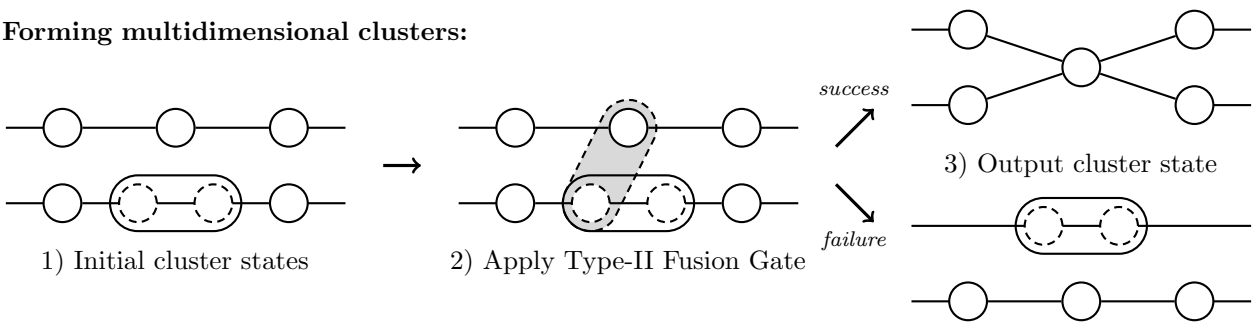

The clear advantage of Type-II fusion over Type-I is the non-destructive nature of the failure outcomes when attempting to build multidimensional clusters. In general this advantage outweighs Type-II's disadvantage of additional qubit consumption per gate and the need redundantly encoded qubits, since dealing with breaks

[5]Here we cannot simply refer to the gates' actions on qubits since the failure modes do not correspond to qubits in the dual rail encoding picture.

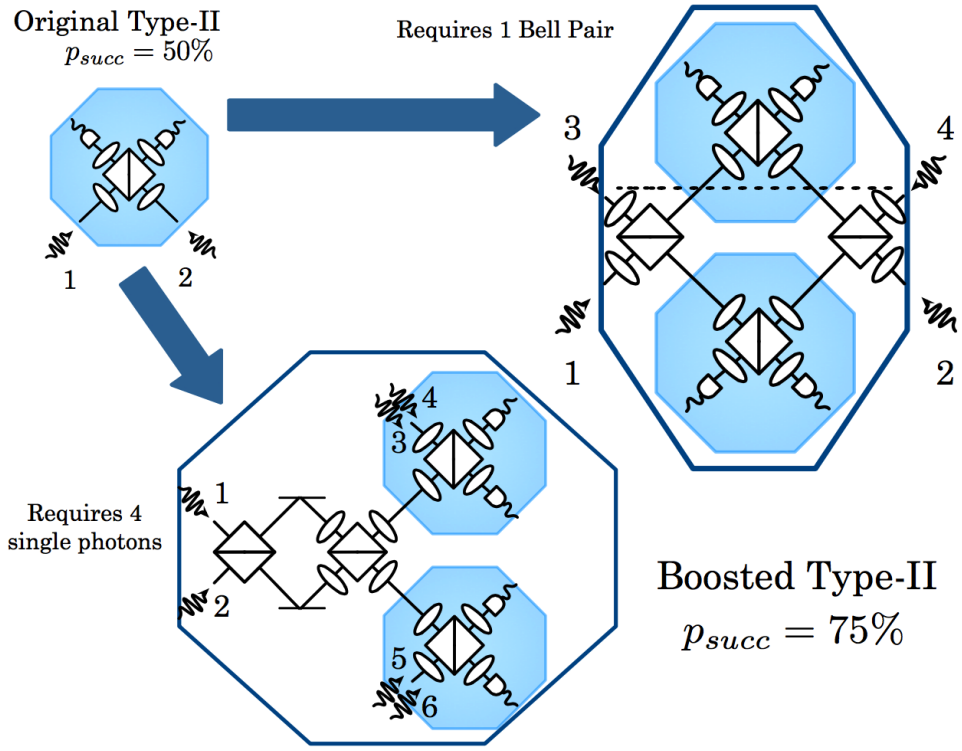

Figure 2: The two forms of boosted Type-II fusion gates for polarisation encoded photonic qubits [7–9].

in large structures is much more problematic. Furthermore, through the additional consumption of entangled Bell pairs or ancillary photons, one can asymptotically boost the probability of success for Type-II fusion, (e.g. $p_{\text{succ}} = 75\%$ can be acheived by consuming a single Bell pair or 4 unentangled ancilla photons, as shown in Figure 2). For these reasons modern cluster state generation protocols usually utilise Type-II fusion.

Another important property of Type-II fusion is it's loss-tolerance, that is, if loss occurs during operation it is detected and hence can be dealt with. Often this is treated as an additional gate failure after which the input states discarded. However, more sophisticated gate operation may be able to utilise this information for other means. This cannot be achieved through Type-I fusion as one cannot distinguish between a failed gate operation with single qubit loss and correct operation without.

4.3 GHZ state generation

When building large cluster states one aims to start with a single, simple, highly reproducible resource state from which the whole state can be constructed. Most modern schemes have focussed on the 3 qubit linear cluster state which is LC-equivalent to a GHZ state[6] (where $|GHZ\rangle = \frac{1}{\sqrt{2}}(|000\rangle + |111\rangle)$) [7, 11]. For linear optical implementations, GHZ states can be created with $p_{\text{succ}} = 1/32 \approx 3\%$, using a combination of Type-I and -II fusion operations, as depicted in the polarisation basis ($|0\rangle = |H\rangle$, $|1\rangle = |V\rangle$) by Figure 3.

An important property of this GHZ production method is that the states produced are independently degraded (ID). This property requires that any loss in the output channels is uncorrelated, and can therefore be modelled as a standard loss channel. This is important as the loss encoding scheme discussed in Section 5 is less tolerant to correlated errors. On success the outputted ID-GHZ state has a loss rate f given by

$$f = 1 - \frac{\eta_S}{2 - \eta_D \eta_S} \,. \tag{5}$$

where η_S and η_D are the single photon source and number resolving detector efficiencies respectively. From

[6]The most obvious exception being the recent Zaidi et al. scheme with a fully connected 3 qubit cluster resource state, requiring an additional CZ cluster link [10].

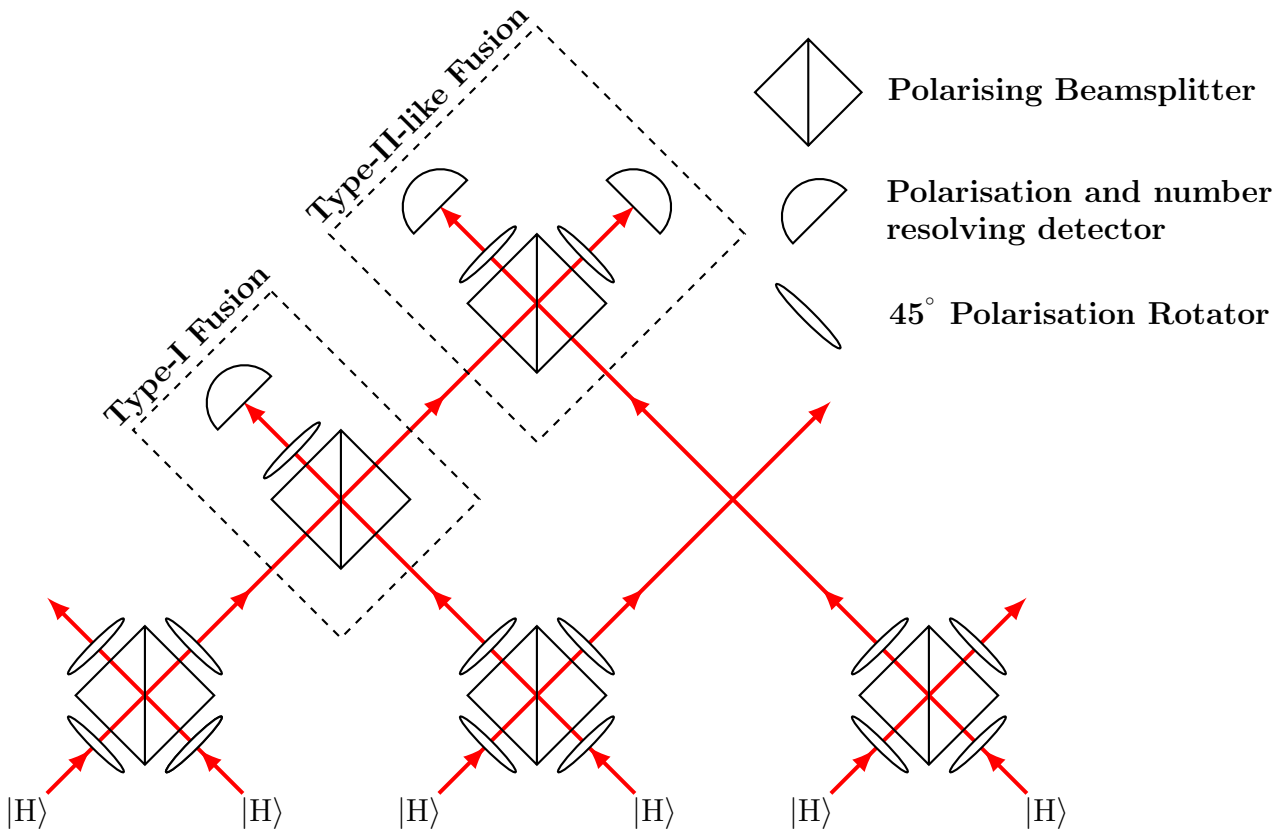

Figure 3: The setup for linear optical generation of ID-GHZ states with $p_{\text{succ}} = 1/32 \approx 3\%$. On success the state is polarisation encoded in the three unattenuated modes, one qubit in each. Here "Type-II-like" refers to the lack of 45° polarisation rotators on the input modes compared the setup depicted in Figure 1b). Image adapted from [4].

this the full output ID-GHZ mixed state is given by

$$\begin{aligned}\rho_{\text{ID-GHZ}} = &(1-f)^3|GHZ\rangle\langle GHZ| \\ &+ \frac{(1-f)^2 f}{2}\left(|H_1H_2\rangle\langle H_1H_2| + |V_1V_2\rangle\langle V_1V_2| + \ldots + |V_2V_3\rangle\langle V_2V_3|\right) \\ &+ \frac{(1-f)f^2}{2}\left(|H_1\rangle\langle H_1| + |V_1\rangle\langle V_1| + \ldots + |V_3\rangle\langle V_3|\right) \\ &+ f^3|vac\rangle\langle vac| \end{aligned} \tag{6}$$

where here $|GHZ\rangle = \frac{1}{\sqrt{2}}\left(|H_1H_2H_3\rangle + |V_1V_2V_3\rangle\right)$ and $|vac\rangle$ is the zero-photon vacuum state for all three modes.

5 Loss tolerant encoding using cluster trees

Whilst toric surface codes can theoretically account for up to 50% qubit loss [1,2], practically this upper bound is likely to be unachievable. For photonic applications however, higher dimensional Raussendorf lattices [12–14] are used, with even lower loss tolerances at 24.9% [3]. Such a tolerance also assumes no computational Pauli errors, for which one has to reduce the tolerable loss rate even further, as shown in Figure 4. This, in addition to other requirements such as: deterministic fusion operations, lossless cluster state creation and that all losses are detectable, further decreases the ability to absorb all losses into the natural loss tolerance of the topological lattice. It is therefore thought that, for photonic applications (in which loss is the predominant form of error), an additional layer of loss encoding is needed.

The scheme we shall discuss below was developed by Varnava, Browne and Rudolph and is known as "counterfactual error correction" [4, 15–17]. This scheme can theoretically encode against up to 50% loss using tree graph states and an "indirect" measurement protocol. This method produces an effective loss rate per qubit on the level of the Raussendorf lattice by encoding each in a tree substructure. This substructure can then be used to measure the original qubit state, even in the presence of high loss. By increasing the size of the trees one

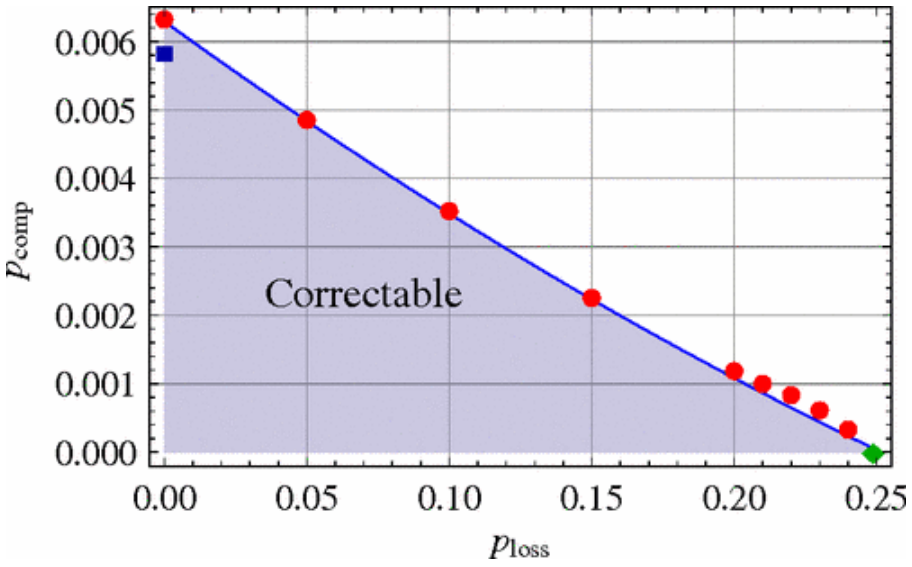

Figure 4: The shaded region depicts levels of loss p_{loss} and computational error p_{comp} which can be tolerated and hence corrected for by a quantum error corrected Raussendorf lattice [3].

can then arbitrarily reduce the effective loss rate to level accommodated by the topological code (or as low as one desires).

5.1 Indirect Measurements

Firstly, it is important to understand the concept of indirect measurements on cluster states. This technique utilises on the correlation information provided by a state's stabilizers. Each stabilizer gives us a description of the different measurement correlations present in a state. For example, consider the three qubit linear cluster state vector

$$\begin{aligned}\left|\Psi_3^{\text{lin}}\right\rangle_{123} &= \frac{1}{\sqrt{2}}\Big(|{+}0{+}\rangle + |{-}1{-}\rangle\Big)_{123} \\ &= \frac{1}{2}\Big[|{+}\rangle_2\Big(|00\rangle + |11\rangle\Big)_{13} + |{-}\rangle_2\Big(|01\rangle + |10\rangle\Big)_{13}\Big] \\ &= \frac{1}{2}\Big[|{+}\rangle_2\Big(|{+}{+}\rangle + |{-}{-}\rangle\Big)_{13} + |{-}\rangle_2\Big(|{+}{+}\rangle - |{-}{-}\rangle\Big)_{13}\Big] \end{aligned} \tag{7}$$

which is stabilized by $\text{Stab}\{\left|\Psi_3^{\text{lin}}\right\rangle\} = \{X_1Z_2, Z_1X_2Z_3, Z_2X_3\}$. While it may not have been apparent previously, we can quickly see that stabilizers give us information on the state's measurement correlations. Firstly, from the state vector, we can see a Z_2 measurement allows us to infer the outcomes of subsequent X_1 and X_3 measurements. This is equally represented in the stabilizer formalism, with post-measurement stabilizers $\{(-1)^{m_2}X_1, (-1)^{m_2}Z_2, (-1)^{m_2}X_3\}$, describing the state of three unentangled qubits, the exact state of each given by m_2. Equally, we can see that an X_2 measurement provides us information on the correlation of the remaining qubits, with post-measurement stabilizers $\{(-1)^{m_2}X_2, X_1X_3, (-1)^{m_2}Z_1Z_3\}$. Now we can easily infer the correlations of the remaining two qubits in both the X and Z measurement bases (given m_2 for the Z case).

In general, given the stabilizer associated with a graph state node $S_j = X_j \prod_{k\in n(j)} Z_k$, the measurements X_j and Z's on all qubits bar one will effectively measure the remaining qubit. It is this observation allows us to perform indirect measurements, even on qubits which have been 'lost'.

5.2 Counterfactual Error Correction

To make use of this indirect measurement technique, tree-shaped cluster state are used. In graph theory, a tree is defined by branching parameters $b = \{b_0, b_1, b_2, \ldots, b_m\}$, giving the number of child nodes per parent node at each layer. An example tree is given in Figure 5. This structure allows for multiple indirect measurements to be attempted in the presence of loss.

The top node the tree is then linked to the lattice qubit in question (either through a direct CZ, or some fusion operation involving redundantly encoded nodes), after which both are measured in the X basis. This removes both qubits, leaving each child node (in the first layer) linked to the lossy qubit's neighbouring nodes. This process is depicted in Figure 6.

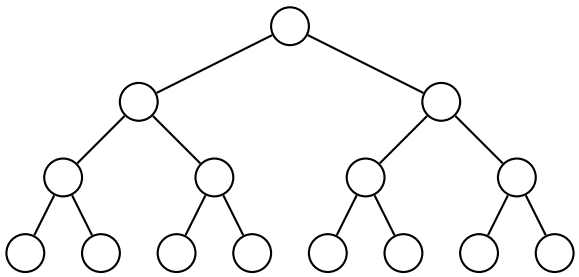

Figure 5: An example of a cluster state tree with branching ratio $b = \{2, 2, 2\}$.

With such a tree substructure connected, one now can attempt operations and measurements on the first layer of qubits. Now in the presence of loss (i.e. a measurement is attempted, but no photons actually detected), one can perform an indirect Z measurement on the lost qubit to remove it from the cluster, and try again on the next first layer node. Upon successful measurement, the rest of the cluster can then be removed. For example, to perform the general measurement $A = \cos\alpha X + \sin\alpha Y$, the procedure is shown in Figure 7. This technique is known as *counterfactual error correction*.

For a tree with branching parameters $\{b_0, b_1, b_2, \ldots, b_m\}$, the probability of successfully performing the measurement A (including removing excess cluster state) is given by

$$P = [(1 - \varepsilon_0 + \varepsilon_0 R_1)^{b_0} - (\varepsilon_0 R_1)^{b_0}](1 - \varepsilon_0 + \varepsilon_0 R_2)^{b_1} \tag{8}$$

where for $k \leq m$

$$R_k = 1 - [1 - (1 - \varepsilon_0)(1 - \varepsilon_0 + \varepsilon_0 R_{k+1})^{b_{k+1}}]^{b_k} \tag{9}$$

and $R_{m+1} \equiv 0$, $b_{m+1} \equiv 0$. Here R_i are the probabilities of successfully performing an indirect Z measurement on any node in the ith level and ε_0 is the raw loss rate. From this we can define the encoded qubit's effective loss rate $\varepsilon_{\text{eff}} = 1 - P$.

5.3 Loss Tolerance

Firstly it can be shown that the effective loss rate (for uncorrelated loss) can only be reduced for $\varepsilon_0 < 50\%$ using cluster trees. This can be intuitively understood by proof by contradiction using the no-cloning theorem. To see this consider Alice and Bob share a four qubit linear cluster, Alice with the first three, Bob the last, which he encodes in a tree-cluster as depicted in Figure 8. Alice can now prepare Bob's encoded qubit in an arbitrary state using the MBQC protocol described in Section 2. Now consider a third party, Charlie, who steals 50% of Bob's qubits at random. Such an act is indistinguishable to a 50% loss rate. If this loss tolerant protocol allowed for recovery of the original state for 50% or greater loss, then both Bob and Charlie could recover and measure Bob's arbitrary state, hence violating the no-cloning theorem.

For $\varepsilon_0 < 50\%$ however, one can show that for a given ε_{eff}, the number of qubits required $Q = \text{polylog}(\frac{1}{\varepsilon_{\text{eff}}})$ and hence the encoding is an efficient one. Given a known ε_0 and desired ε_{eff}, a numerical search over branching parameters can be found for the optimal tree cluster to use, with results shown in Figure 9. The aforementioned

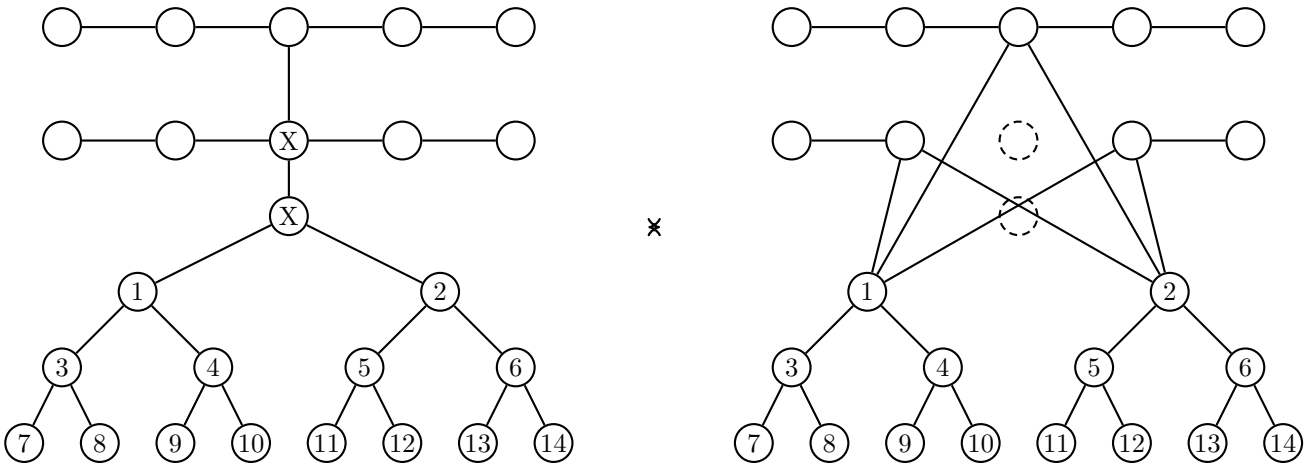

Figure 6: A loss encoded qubit using a cluster tree. For brevity, the left hand side image is used to denote the highly-connected post-measurement cluster. Numbers are included for reference by Figure 7.

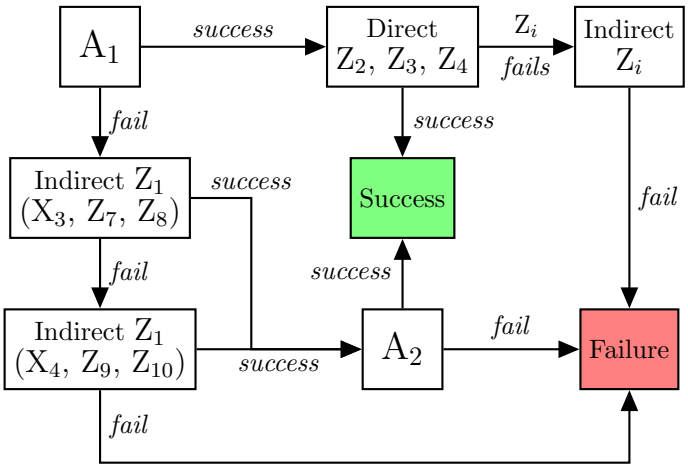

Figure 7: The process flow for performing a measurement A on the encoded qubit. Here *fail* indicates that qubit has been lost (and hence cannot be measured). Also note that on failure, one may still be able to attempt to remove the encoded qubit from the larger lattice to prevent further errors occurring.

upper limit on loss tolerance was also confirmed, with the numerical search also finding no advantage provided by tree-clusters for $\varepsilon_0 \geq 50\%$.

Lastly, by noting that the ID-GHZ loss rate f and loss threshold $\epsilon < \frac{1}{2}$ are related by

$$(1-f)\eta_D = 1 - \epsilon \tag{10}$$

one can use equation 5 to show that such loss tolerance can be achieved for

$$\eta_S \eta_D > \frac{2}{3}\,, \tag{11}$$

providing a hard theoretical limit on the equipment needed for such a protocol.

5.4 Efficient Tree Construction

Such an encoding scheme can only be of practical use if it can be implemented *efficiently*. This efficiency refers specifically to the construction of trees, which in linear optical schemes requires the use of probabilistic fusion gates.

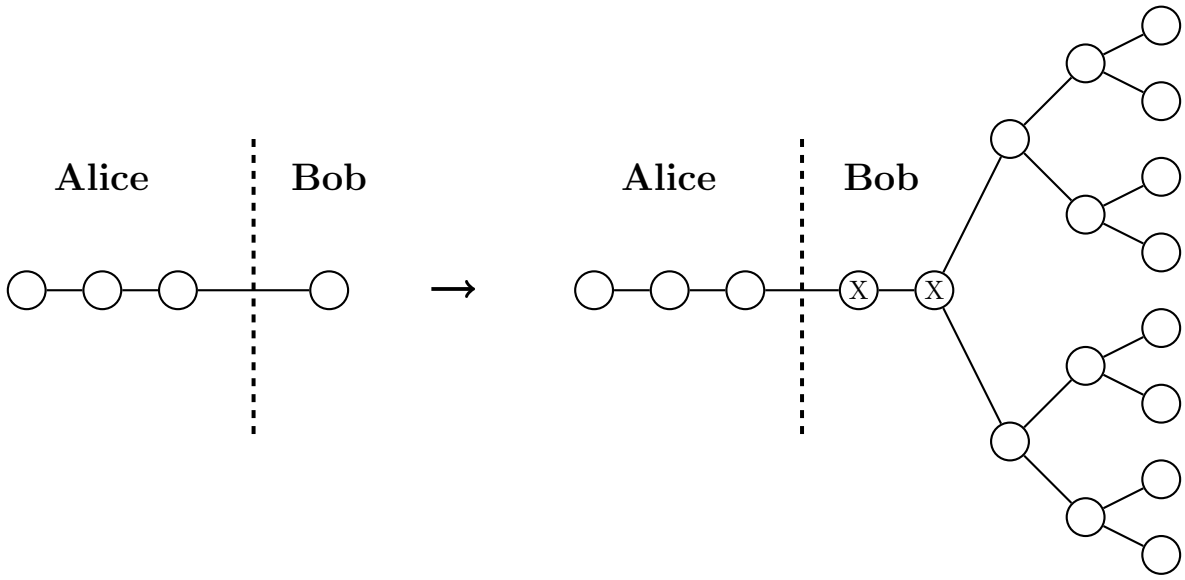

Figure 8: A visual aid to help prove the upper bound on cluster tree efficacy via a no-cloning contradiction. See text for argument.

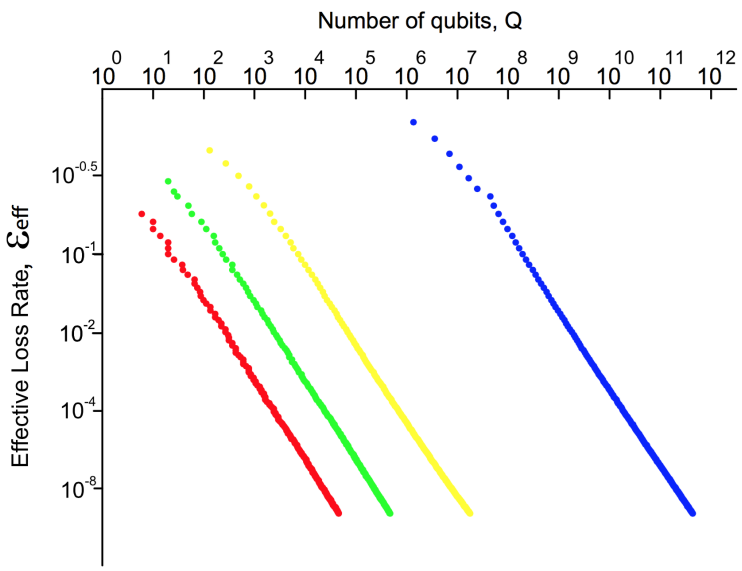

$\{b_i, b_2 ... b_m\}$	Q	ε_0	ε_{eff}
$\{2, 3, 2\}$	20	20%	10^{-1}
$\{4, 5, 6, 1\}$	264	20%	10^{-2}
$\{5, 10, 9, 1\}$	955	20%	10^{-3}
$\{7, 15, 11, 1\}$	2422	20%	10^{-4}
$\{8, 22, 14, 1\}$	5112	20%	10^{-5}
$\{3, 6, 6, 1\}$	237	30%	10^{-1}
$\{5, 21, 11, 1\}$	2420	30%	10^{-2}
$\{7, 19, 22, 2\}$	8918	30%	10^{-3}
$\{9, 30, 29, 2\}$	23769	30%	10^{-4}
$\{11, 23, 22, 4, 1\}$	50358	30%	10^{-5}
$\{4, 27, 22, 2\}$	7240	40%	10^{-1}
$\{6, 26, 34, 6, 1\}$	69114	40%	10^{-2}
$\{9, 36, 53, 7, 1\}$	2.58×10^{5}	40%	10^{-3}
$\{12, 43, 78, 8, 1\}$	6.85×10^{5}	40%	10^{-4}
$\{14, 48, 114, 9, 1\}$	1.46×10^{6}	40%	10^{-5}
$\{5, 27, 45, 61, 39, 6, 1\}$	2.17×10^{8}	49%	10^{-1}
$\{8, 45, 77, 105, 45, 7, 1\}$	1.97×10^{9}	49%	10^{-2}
$\{12, 59, 113, 133, 47, 7, 1\}$	7.51×10^{9}	49%	10^{-3}
$\{15, 76, 140, 169, 50, 7, 1\}$	2.03×10^{10}	49%	10^{-4}
$\{19, 97, 172, 186, 51, 7, 1\}$	4.52×10^{10}	49%	10^{-5}

Figure 9: Numerical results for the efficacy of tree clusters at reducing effective loss rates [4]. The different plots, from left to right correspond to $\varepsilon_0 = 20\%$, 30%, 40% and 49%. Here ε_0 and ε_{eff} denote the raw and the tree-encoded effective loss rates respectively. For a fixed ε_0 and ε_{eff}, a numerical search was performed over branching parameters $\{b_0, b_1, b_2, \ldots, b_m\}$ to minimise Q. This result indicates that $Q = \text{polylog}(\frac{1}{\varepsilon_{\text{eff}}})$.

Firstly, however, we must construct a repeatable procedure for arbitrary tree construction. Here the fundamental building block is the 2-tree: a redundantly encoded qubit with two child nodes. These can be constructed from GHZ states as follows:

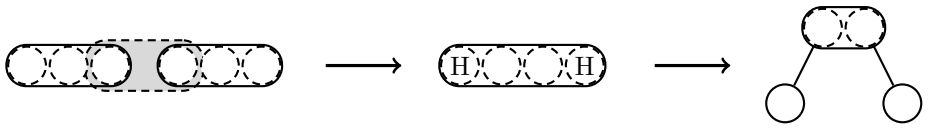

1) Fuse two GHZ states 2) Apply Hadamards 3) 2-tree created

To increase the branching parameter for a given node, trees are then fused together at the top level:

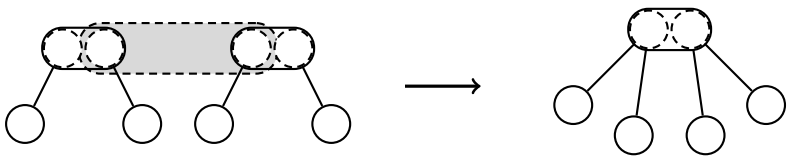

1) Fuse 2-trees at top layer 2) Branches added

To add a layer, trees are fused from top to bottom:

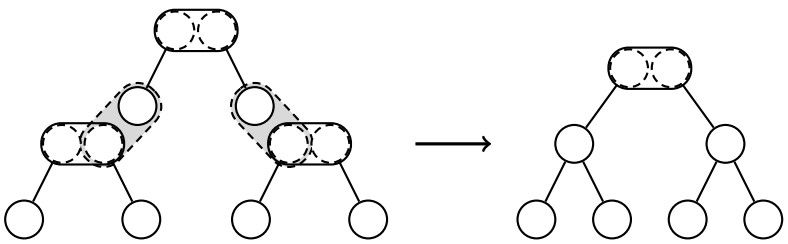

1) Fuse 2-trees top to bottom 2) Layer added

where in all the above cases, Type-II fusion has been used. By repeating these simple operations a tree of any dimensions can theoretically be built.

However, such a scheme must accommodate the probabilistic nature of fusion operations as well as inherent loss rates. The most basic protocol for tree building simply discards both input states when either gate failure

or loss occur, restarting construction afresh. Whilst in reality this would seem an incredibly inefficient way to produce each tree, if we can show a efficient scaling for this method, then there is scope for development of more sophisticated construction schemes.

Firstly, the success rate for (unboosted) Type-II fusion is given by

$$P_{II} \equiv \frac{1}{2}\left(1 - \frac{\eta_D \eta_S}{2 - \eta_D \eta_S}\right)^2 \tag{12}$$

where the factor of $\frac{1}{2}$ is the gate's base rate of success and $\left(1 - \frac{\eta_D \eta_S}{2-\eta_D \eta_S}\right)^2$ gives probability of both photons both being present in the cluster state (given by equation 5) and then detected correctly (with probability η_D). The cost of creating a 2^l-tree (a redundantly encoded qubit with 2^l child nodes) is $\frac{2}{P_{II}}$ 2^{l-1}-trees or equivalently $(\frac{2}{P_{II}})^{l-1}$ 2-trees. Furthermore to construct a b_m-tree where $2^{l-1} \leq b_m \leq 2^l$, the average number of 2-trees required is

$$\leq \left(\frac{2}{P_{II}}\right)^{\log_2(b_m)} = \text{poly}(b_m)\ . \tag{13}$$

To add another layer of branching parameter b_{m-1} two of the above b_m-trees are fused top to bottom with a 2-tree, thus incurring a cost factor of $\left(\frac{2}{P_{II}}\right)^2$. Many of these states are thus created and subsequently fused at the top level to produce the desired $\{b_{m-1}, b_m\}$ cluster tree (with a redundantly encoded top qubit). The average 2-tree cost of creating such a state is

$$\leq \left(\frac{2}{P_{II}}\right)^{\log_2(b_{m-1})} \left(\frac{2}{P_{II}}\right)^2 \text{poly}(b_m) = \left(\frac{2}{P_{II}}\right)^2 \text{poly}(b_{m-1})\text{poly}(b_m)\ . \tag{14}$$

By iterating this procedure to produce the desired $\{b_0, b_1, \ldots, b_m\}$ tree, the average number of 2-trees required is

$$\langle N_{\text{2-trees}} \rangle \leq \left(\frac{1}{P_{II}}\right)^{2m} \prod_{i=0}^{m} \text{poly}(b_i)\ . \tag{15}$$

Therefore to construct a tree of Q qubits only requires poly(Q) qubits since it can be shown that $m \leq \log_2(Q)$ holds for any Q qubit tree. We can thus conclude that (in the asymptotic limit), such loss-tolerant trees can be built efficiently.

The final step in the above protocol is to link the cluster trees encoded qubits together to produce the desired topological lattice. Having encoded each qubit in a cluster tree one can attempt to fuse together top layer qubits from each. On success this connects the encoded qubits to form the desired lattice, whereas failure can be counted as loss and the fusion reattempted.

5.5 Tolerance to other errors

One immediate issue that many loss-tolerant protocols face is the unintentional exacerbation of Pauli errors, that is bit flip and phase errors. These can be modelled as X or Z operations randomly applied to the susceptible qubits. Given the highly entangled nature of these cluster tree states, one may expect such errors to heavily accumulate, rendering such a scheme useless. However for counterfactual error correction this is not necessarily the case.

Firstly, the encoded qubit's exposure to errors is due to the whole cluster tree. This is due to the scheme's natural level of redundancy, as during operation not all qubits have to be measured. For example, to encoded for $\varepsilon_{\text{eff}} = 10^{-10}$ with an initial loss rate $\varepsilon_0 = 0.2$, then non Pauli measurements will be attempted on at most 15 of the qubits in each tree [15]. Furthermore the majority of operations here are in the Clifford group, for which fault-tolerant implementations are known [18].

However for Pauli errors that do occur through erroneous indirect measurements, one can significantly reduce their impact by implementing a majority voting protocol. In this scheme Pauli errors are overcome by repeating the indirect measurement using the other branches and taking the majority result for the phase correction.

Unfortunately the above redundancy and majority voting arguments do not hold for errors on the top level of qubits. For these additional error-correction encoding is required. The most suitable for this would be the 15-qubit quantum Reed-Muller code [19], since it is the only known code where non-Pauli measurements on encoded qubits can be made with single qubit measurements [4, 12].

Lastly, we have yet to consider loss on the tree's top qubits, assumed to have been faultlessly measured in the X basis. Such loss errors can be simply incorporated into the probabilistic process of tree generation. Alternatively one could attempt to build the desired post-measurement state (shown in Figure 6) directly.

6 Conclusion

During this report we have introduced the loss-tolerance scheme known as counterfactual error correction, as well as the supporting theoretical framework. This framework includes: measurement-based quantum computation; the cluster state picture; the stabilizer formalism; and cluster state construction. The scheme itself provides an efficient method for encoding lossy qubits using cluster trees (of similarly lossy qubits), to produce a reduced effective loss rate for raw loss rates $\varepsilon_0 < 50\%$. This is a proof of principle design showing that LOQC can be theoretically achieved even in the presence of significant loss, perhaps providing a feasible solution for near-future implementations. While much work still needs to be done on reducing substrate material loss rates, this provides a tangible target, at which this scheme can be applied.

However, even if such loss rates are reached, work is still required to bring this scheme into practical maturity. Most obviously, the initially proposed method of construction clearly leaves much room for optimisation. This may simply be a method for reusing the previously discarded states from failed fusion attempts, or perhaps a more advanced approach such as percolation methods (as used in modern cluster lattice constructions [7]). Also, ideally any currently practical method would require minimal active switching since this produces much loss in photonic implementations.

Another area for improvement may be found in the optimisation of resource state production, namely for GHZ states. It is currently unknown whether the current rate ($p_{\text{succ}} = 1/32$) for GHZ production is optimal. Regardless of the outcome, it is important for many proposals in LOQC that this limit is known. If an improved method is found then this could significantly increase the feasibility of such proposals. On the other hand, if this is the best that can be achieved, schemes must either accommodate this, or utilise non-passive processes for production or otherwise. There are also implementation-specific optimisations that have yet to be investigated. For example, for linear optical schemes in which certain photons experience more elements than others, one can prioritise or increase encoding on said qubits.

Lastly, it is not know if more efficient loss tolerance protocols can be developed, utilising completely different cluster structures or methods entirely. Above all, this scheme has provided a precedence and paved the way for modern loss tolerant schemes in general. Given the recent advancements in LOQC, the field has taken a reinvigorated interest in such schemes, requiring old stones to be overturned, forgotten avenues to be retrodden and new directions to be explored. With the race to produce the first large scale quantum computer well and truly under way, the challenges have never been greater, the chase never so exciting and rewards never as sweet.

References

[1] T. M. Stace, S. D. Barrett, and A. C. Doherty, "Thresholds for topological codes in the presence of loss," *Physical Review Letters*, vol. 102, no. 20, pp. 1–4, 2009.

[2] T. M. Stace and S. D. Barrett, "Error correction and degeneracy in surface codes suffering loss," *Physical Review A - Atomic, Molecular, and Optical Physics*, vol. 81, no. 2, pp. 1–10, 2010.

[3] S. D. Barrett and T. M. Stace, "Fault tolerant quantum computation with very high threshold for loss errors," *Physical Review Letters*, vol. 105, no. 20, pp. 1–4, 2010.

[4] M. Varnava, *Linear Optics Quantum Computing Tolerant To Qubit Loss*. PhD thesis, 2007.

[5] D. E. Browne and T. Rudolph, "Resource-efficient linear optical quantum computation.," *Physical Review Letters*, vol. 95, no. 1, p. 010501, 2004.

[6] E. Knill, R. Laflamme, and G. J. Milburn, "A scheme for efficient quantum computation with linear optics.," *Nature*, vol. 409, pp. 46–52, Jan. 2001.

[7] M. Gimeno-segovia, P. Shadbolt, D. E. Browne, and T. Rudolph, "From three-photon GHZ states to universal ballistic quantum computation," pp. 1–9, 2015.

[8] F. Ewert and P. van Loock, "3/4-efficient bell measurement with passive linear optics and unentangled ancillae," *Phys. Rev. Lett.*, vol. 113, p. 140403, Sep 2014.

[9] W. Grice, "Arbitrarily complete Bell-state measurement using only linear optical elements," *Physical Review A*, vol. 84, no. 4, pp. 1–6, 2011.

[10] H. Zaidi, C. Dawson, P. van Loock, and T. Rudolph, "Near-deterministic creation of universal cluster states with probabilistic Bell measurements and 3-qubit resource states," *arXiv*, pp. 1–6, 2014.

[11] Y. Li, P. C. Humphreys, and S. C. Benjamin, "Resource costs for fault-tolerant linear optical quantum computing," pp. 1–13, 2015.

[12] R. Raussendorf, J. Harrington, and K. Goyal, "A fault-tolerant one-way quantum computer," *Annals of Physics*, vol. 321, no. 9, pp. 2242–2270, 2006.

[13] R. Raussendorf, S. Bravyi, and J. Harrington, "Long-range quantum entanglement in noisy cluster states," *Physical Review A - Atomic, Molecular, and Optical Physics*, vol. 71, no. 6, pp. 1–6, 2005.

[14] R. Raussendorf and J. Harrington, "Fault-tolerant quantum computation with high threshold in two dimensions," *Physical Review Letters*, vol. 98, no. 19, pp. 1–4, 2007.

[15] M. Varnava, D. E. Browne, and T. Rudolph, "Loss tolerance in one-way quantum computation via counterfactual error correction," *Physical Review Letters*, vol. 97, no. 12, 2006.

[16] M. Varnava, D. E. Browne, and T. Rudolph, "Loss tolerant linear optical quantum memory by measurement-based quantum computing," *New Journal of Physics*, vol. 9, 2007.

[17] M. Varnava, D. E. Browne, and T. Rudolph, "How good must single photon sources and detectors Be for efficient linear optical quantum computation?," *Physical Review Letters*, vol. 100, no. 6, pp. 1–4, 2008.

[18] M. Nielsen and I. Chuang, *Quantum computation and quantum information*. 2010.

[19] S. Bravyi and A. Kitaev, "Universal quantum computation with ideal Clifford gates and noisy ancillas," *Physical Review A - Atomic, Molecular, and Optical Physics*, vol. 71, no. 2, pp. 1–14, 2005.